Theoretical and Experimental Evaluation of a Chain Strength Measurement System for Pedelecs

C. Abagnale, M. Cardone, P. Iodice, S. Strano, M. Terzo and G. Vorraro

***Abstract*— In this paper, a theoretical/experimental analysis of a new measurement system of the chain strength is described. Such system is functional for the control of the electrically assisted bicycles which are characterized by a driving torque due to the contribution of both electric motor and rider. The electrical assistance is commonly regulated taking into account informations such as the chain ring rotation, the bicycle speed and/or the torque given by the rider. As a consequence, suitable measurements have to be made on board in order to handle the assistance performances and to improve drivability.**

***Index Terms*— pedelec, rider effort, chain strength**

I. Introduction

IN the recent years, the increasingly congested traffic has led to reflections on strong problems related both to the air quality and to the use of petroleum [1, 2, 3].

Particularly in the urban centres, fuel consumption and emissions are due to the high number of vehicles on the road, to their average speed and to the total mass of the system "vehicle plus transported". In fact the majority of cars on the road has a mass in the range of 800 to 1600 kg and they often carry one or two people, with a consequent ratio "total mass of the vehicle and transported people" within the range of 12 to 22. This suggests that most of consumption and pollution are attributable to the great mass of the vehicle and not to the mass of handled passengers.

In this context, a vehicle as the e-bike [4]-[6] can be considered a promising alternative vehicle for both personal mobility and goods delivery, especially for small and medium distances. The e-bike, in all its forms, two or three wheels (tricycle), is able to move with an average speed equal to the typical one of the town traffic and, at the same time, it requires energy for its mobility that is very close to the necessary energy just for the displacement of the transported people.

Obviously, the bike is not useful to cover large distances, but the "bike-sharing" can solve the problem ensuring the user the freedom to use a bike and leave it as necessary.

The e-bikes are normally powered by rechargeable battery [7]–[10], and their driving performance is influenced by battery capacity, motor power, road types, operation weight, control, and particularly the management of assisted power.

A classification of these BEVs (battery electric vehicles) is necessary. A first kind is represented by a pure electric bike (e-bike) [11]–[13], which integrates electric motor into bicycle frame or wheels, and it is driven by motor force only using a handlebar throttle. A second kind is a power-assisted bicycle, or called pedelec [14] hereafter, which is a human–electric hybrid bicycle [15] that supports the rider with electric power only when the rider is pedalling. The pedelecs are characterized by a driving torque due to both an electric motor torque and a rider one. As regards the rider torque, two different sensors are usually adopted: the first one is a torsiometer installed in the pedal hub; the second one is a load cell typically installed between the rear wheel and the frame. The first solution is more expensive and requires more space to locate the device while the second solution is a low cost one and very few invasive. On the contrary, the employment of a load cell is not functional to directly measure the rider torque but only the chain strength.

This paper presents a theoretical/numerical analysis and an experimental validation of a new low cost system for the measurement of the chain strength. The device equips a new pedelec prototype and is based on the employment of a load cell and suitable constraints that link the sensor to the bicycle frame, in order to make the measured force as close as possible to the real chain strength. The theoretical and numerical analysis have been realized by means of the modelling of the part of the system in which the load cell is positioned. Experimental results are illustrated in order to validate the proposed solution for the employment on electrically assisted bicycles.

II. The Innovative Solutions for Pedelecs

The low cost measurement system, that will be described

C. Abagnale is with the *Dipartimento di Ingegneria Industriale, Università degli Studi di Napoli Federico II*, Napoli, 80125 ITALY (e-mail: c.abagnale@unina.it).

M. Cardone is with the *Dipartimento di Ingegneria Industriale, Università degli Studi di Napoli Federico II*, Napoli, 80125 ITALY (e-mail: massimo.cardone@unina.it).

P. Iodice is with the *Dipartimento di Ingegneria Industriale, Università degli Studi di Napoli Federico II*, Napoli, 80125 ITALY (e-mail: paolo.iodice@unina.it).

S. Strano is with the *Dipartimento di Ingegneria Industriale, Università degli Studi di Napoli Federico II*, Napoli, 80125 ITALY (e-mail: salvatore.strano@unina.it).

M. Terzo is with the *Dipartimento di Ingegneria Industriale, Università degli Studi di Napoli Federico II*, Napoli, 80125 ITALY, (corresponding author, phone: +390817683277; fax: +390812394165; e-mail: m.terzo@unina.it).

G. Vorraro is with the *Dipartimento di Ingegneria Industriale, Università degli Studi di Napoli Federico II*, Napoli, 80125 ITALY (e-mail: giovanni.vorraro@unina.it).

in the next section, is one of the innovative solutions concerning the new prototype of pedelec. The other ones are:

- the electric motor location;
- the mechanical transmission.

Differently from a common approach, in which the electric motor is located on one of the three hubs of the bicycle, a basic idea of the pedelec prototype consists of a central motor located in a bottle, as shown in Fig. 1, while a gearbox is located in a central position, between the pedals, as pointed out in Fig. 2.

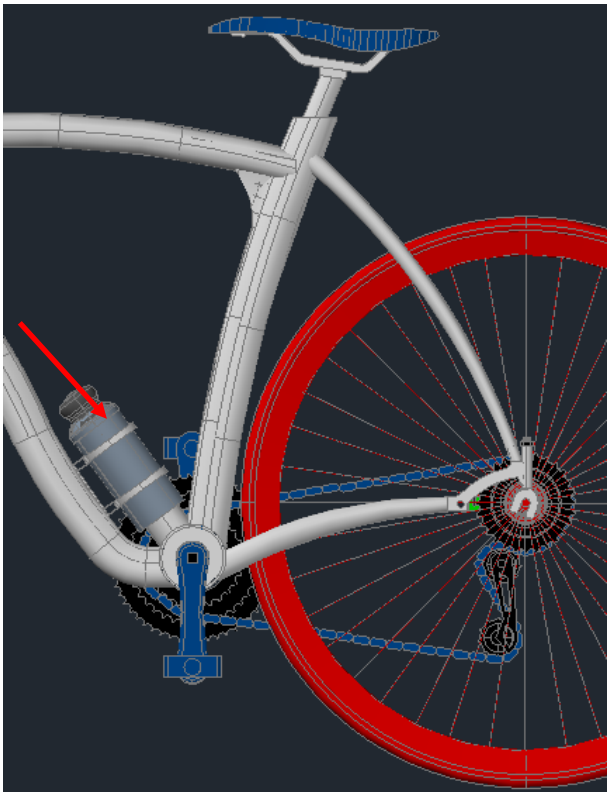

Fig. 1. The electric motor location.

This transmission is not direct, as in almost all the current bikes: a manual gearbox, added to that one usually provided on modern bikes, is useful to make easier to ride uphill (particularly suited to older people and under conditions of non-flat roads).

A detailed description of the proposed measurement system of the chain strength is given in the next section.

III. The Low Cost Measurement System

An important classification of the pedelec is based on the typology of the controller that manages the assistance. As first step, the controllers can be feedforward or feedback ones: the feedforward controller is not based on actions depending on measurements and employs the sensors fundamentally for flag signals (ON/OFF controller); the feedback controller [16, 17] generates an assistance torque that is a function of a signal obtained by measurements. The measurements realized on board depend on the kind of the control and are typically the chain ring rotation, bicycle speed and rider effort. Particularly, as regards the feedback controller, the rider effort is often required. Indeed, in this kind of controlled assisted bicycles, the contribution to the traction force of the vehicle by the electric motor can be made proportional to the contribution of the cyclist. For instance, the motor could be controlled in order to double the effort made by the cyclist. Moreover, the distribution between the motor power and the human power can further be controlled as function of other informations (speed, different assistance modes selected by the user).

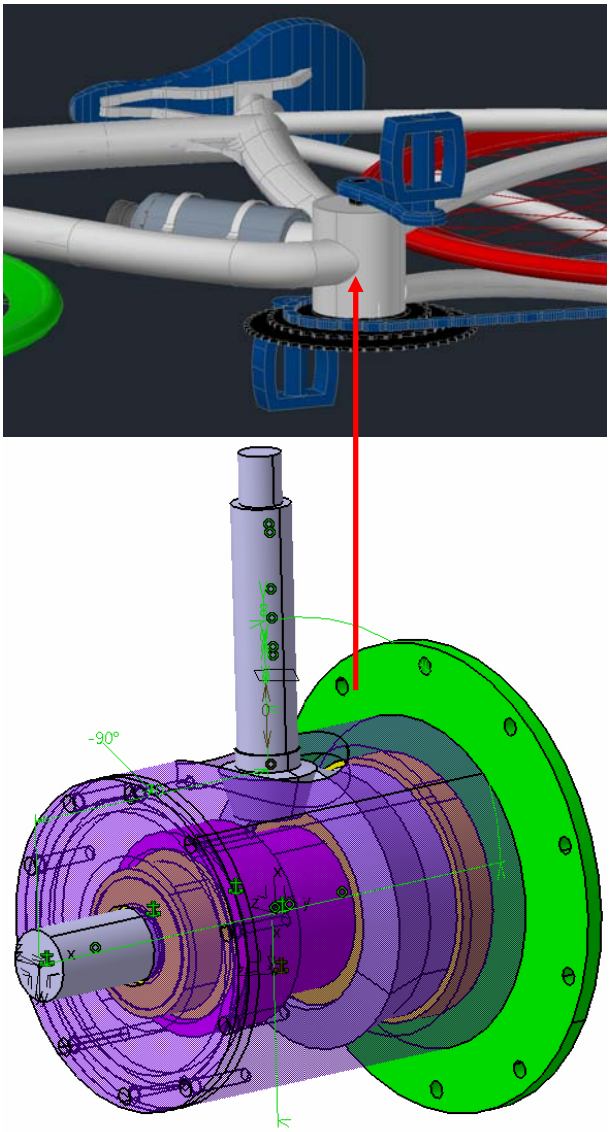

Fig. 2. The gearbox on the pedelec.

With reference to the measurements of the rider effort, two different devices are often employed. A first measurement system consists of a torsiometer mounted on the pedal hub [18]. Instead, a second device is based on a Hall effect sensor useful to measure the chain strength and located between the rear wheel hub and the frame [19].

As introduced above, this paper presents a measurement system of the chain strength characterized by a cost approximately equal to half of that of the two mentioned devices. It is based on a strain gauge load cell located on one side of the rear wheel, between the hub and the frame (Fig. 3, 4).

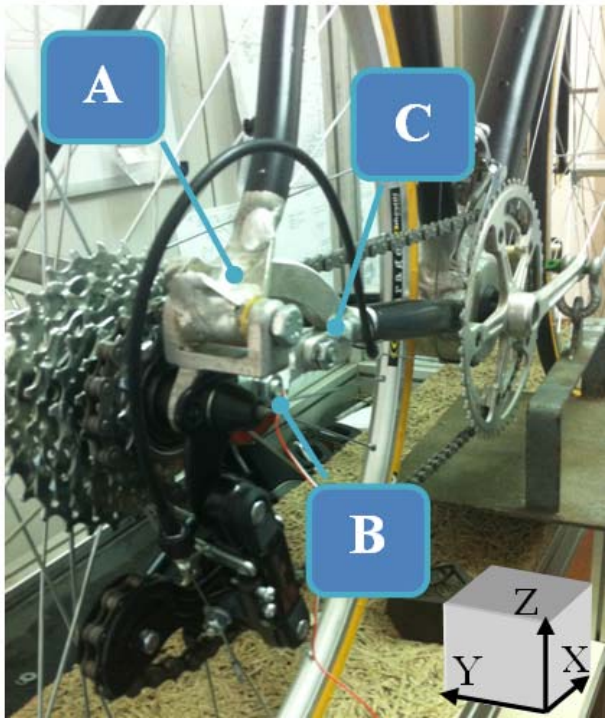

Fig. 3. The measurement system.

On the other side of the wheel, a hinge constraint has been adopted (Fig. 5) in order to allow rotation in a plane parallel to the road surface. The strain gauge load cell is linked to the frame and to the hub by means of three hinges (A, B and C in Fig. 3, 4) in order to make the load applied to the load cell as close as possible to the chain strength.

With reference to the rear wheel of the bicycle, the following actions can be observed along the longitudinal direction (Fig. 6):

- the chain strength T;
- the tyre-road longitudinal force F_x;
- the frame reaction V.

The crown radius and the wheel radius have been represented with r and R respectively.

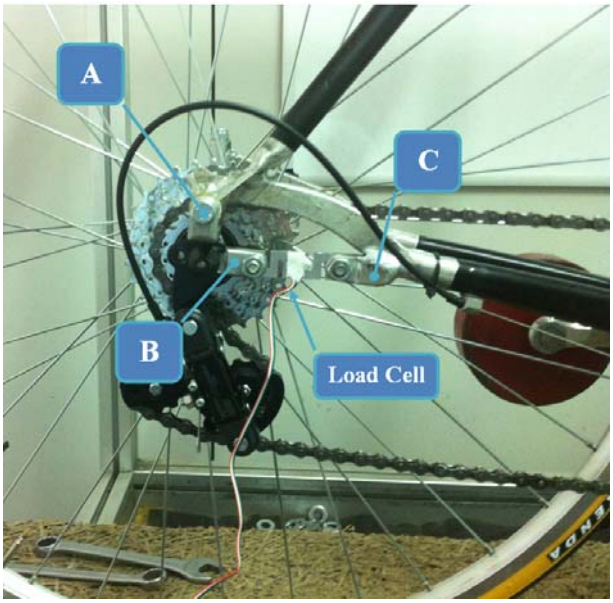

Fig. 4. Detail of the strain gauge load cell.

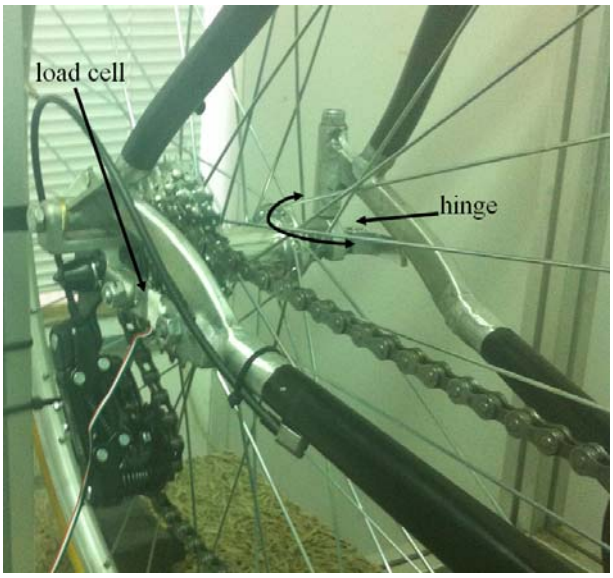

Fig. 5. Detail of the measurement system.

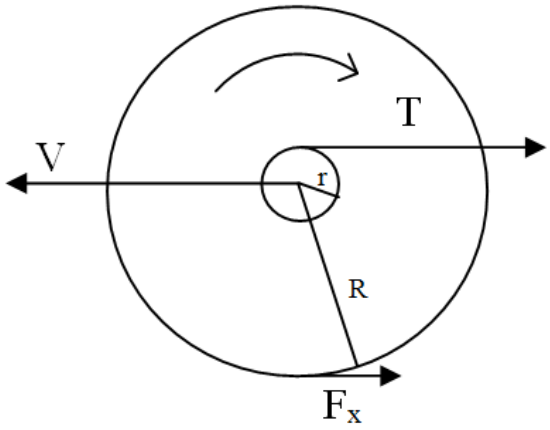

Fig. 6. Schematic representation of the driving wheel.

Taking into account the rotation and translational equilibrium, it can be written:

$$I\ddot{\vartheta} = F_x R - Tr \tag{1}$$

$$F_i + V = T + F_x \tag{2}$$

where I, $\ddot{\vartheta}$, F_i are the wheel moment of inertia, the wheel angular acceleration, and the longitudinal inertial force respectively.

Due to the reduced inertial loads of the wheel bicycle and being r<<R, T can be considered much greater than F_x and so, the frame reaction V is substantially equal to the chain strength T. Moreover, the load cell is mounted on the side of the frame in which the crown is located: with reference to a plane parallel to the (x,y) one (Fig. 7), the chain strength T is almost totally balanced by the cell (a<<b).

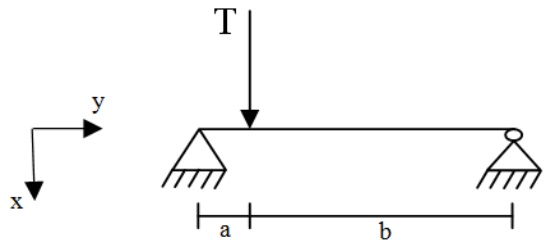

Fig. 7. Schematic representation in the (x,y) plane.

Such consideration exhorts to employ gears, differently from the illustrated images, not based on derailleur, in order to have a small fixed value of the "a" dimension.

With reference to the (x, z) plane (Fig. 3), the measurement system can be represented as in Fig. 8:

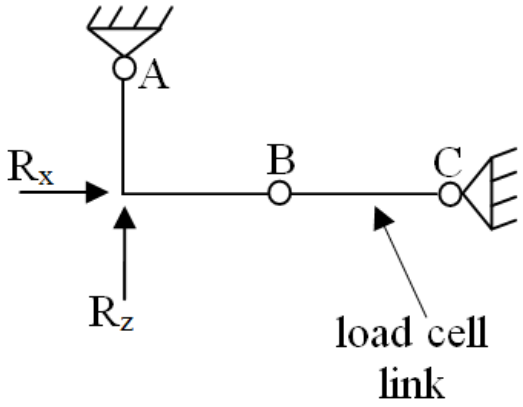

Fig. 8. Schematic representation of the measurement system.

in which the forces R_x and R_z are, respectively, the actions due to the presence of the chain strength T and the tyre-road vertical force. A contained dimension of "a" and the presence of a suitable hinge in the (x, y) plane (Fig. 5, 7) are fundamental to make the chain strength T very close to the force R_x.

The three hinges introduced above (A, B and C) have been illustrated in Fig. 8: their presence allows to consider the force R_x loading the load cell represented as the link between the points B and C. At the same time, the vertical load R_z, under the hypothesis of reduced slope of the road, is not characterized by component along the x direction and, consequently, does not represent a disturb for the measurement of the chain strength. Conversely, the presence of a slope causes a component of the vertical load acting on the load cell that is, in any case, well accepted because it determines an overestimation of the chain strength, and, as a consequence, an increased assistance torque due to the proportional contribution.

IV. Numerical Analysis

In this section, a multi-body model of the bike is presented. The purpose of this analysis is to verify, in simulation environment (Working Model), the relationship between the actual chain strength and the measurement obtained with the load cell. A two-dimensional analysis has been considered, and then, bodies, constraints, and forces refer to the (x,z) plane (Fig. 3). Moreover, all the simulation results have been obtained in static condition.

Fig. 9 shows the scheme of the multi-body model, in which two ground parts (vertical and horizontal) have been adopted. The bike is composed by the frame, the two wheels, the front and the rear crowns (represented by two yellow circle), the pedal and the measuring system of the chain force.

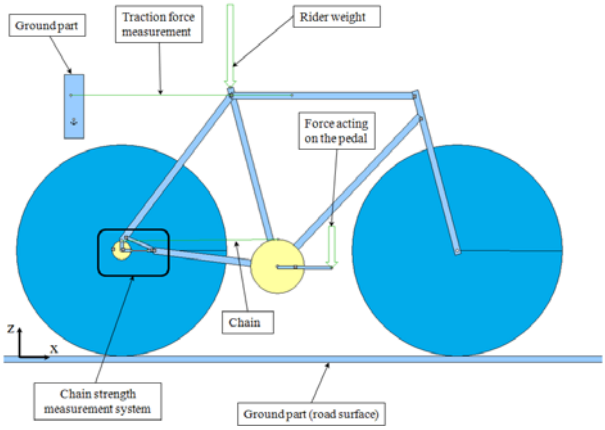

Fig. 9. Scheme of the multi-body bike model.

With reference to Fig. 9, the chain has been modelled using a rigid rod that connects two points of the front and rear crowns, respectively. Another rigid rod has been used to simulate the presence of the a traction force measurement sensor.

The wheels are connected to the frame by two revolute joints and the contacts between the wheels and the road surface have been imposed. The front crown is connected to the frame with a revolute joint, while the rear crown is rigidly fixed to the rear wheel.

The pedal is rigidly connected to the front crown. Moreover, the weight of the rider and his action on the pedal have been applied. Fig. 10 shows in detail the system for measuring the chain force.

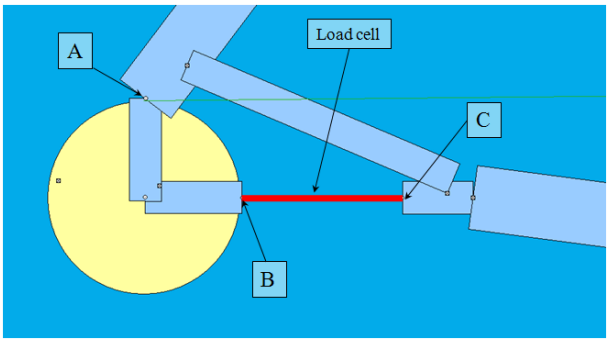

Fig. 10. Scheme of the chain strength measurement system.

In Fig. 10, the main system connections are indicated with the same letters of Fig. 8. The load cell has been modelled with a rigid rod element, which simulates a typical

very high stiffness characterizing this kind of sensor. Simulations have been carried out and the results are summarized in Table I. All the tests have been performed considering only the bicycle weight and, therefore, the model input is the force acting on the pedal (Applied load). The outputs are the forces acting on the rigid rods representing the chain (Chain strength), the proposed measurement system (Measurement) and the traction force measurement system (Tyre-road interaction).

TABLE I
NUMERICAL RESULTS

Applied load (N)	Chain strength (N)	Tyre-road interaction (N)	Measurement (N)
21.6	43.2	3.9	47.1
31.4	62.8	5.7	68.5
41.2	82.4	7.5	89.9
60.8	121.6	11.1	132.7
80.4	160.9	14.6	175.5
109.9	219.7	20.0	239.7
129.5	259.0	23.6	282.6
158.9	317.8	28.9	346.7

Since the simulations have been conducted in static conditions, the inertial force is null, and therefore the force V in (2) is balanced by the sum of the tyre-road interaction F_x and the chain strength T. The results of the numerical analysis reported in Table I highlight that the proposed measurement system gives the force V; indeed, in accordance with (2), the values of the fourth column are equal to the sum of the corresponding values of the second and third columns. In any case, it can be observed that the tyre-road interaction is substantially much less than the chain strength (Fig. 11) and, consequently, the measurement value can be considered very close to the chain strength itself (Fig. 12).

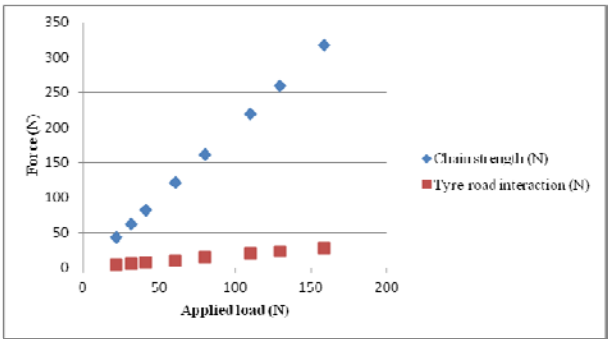

Fig. 11. Comparison between the chain strength and the tyre-road interaction.

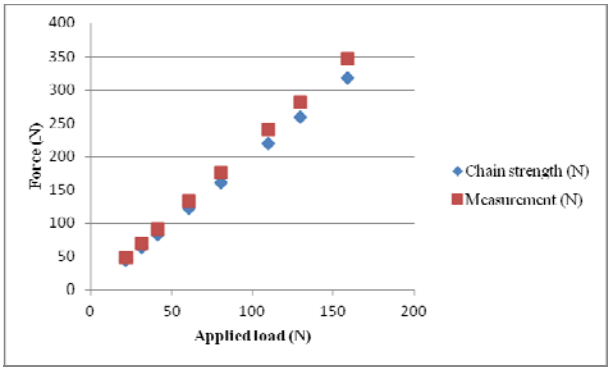

Fig. 12. Comparison between the chain strength and the measurement.

Fig. 13 shows the linear behaviour concerning the input-output relationship of the measurement respect to the chain strength.

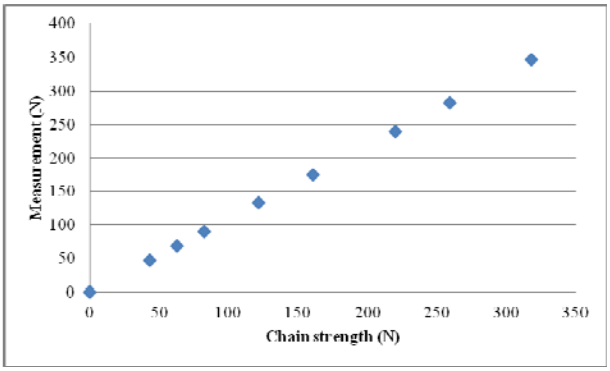

Fig. 13. Measurement vs chain strength.

In order to better understand the performances of the proposed measurement system, experimental results are proposed in the next section, using the same inputs adopted for the numerical simulations.

V. EXPERIMENTAL ANALYSIS

Experimental tests have been realized in order to validate the proposed measurement system. To this aim, the bicycle has been linked to a suitable frame (Fig. 14) by means of a supplemental load cell (Fig. 15).

Fig. 14. The test rig.

Fig. 15. Additional load cell.

The application of known loads in correspondence of the pedals determines the longitudinal tire-road force F_x, balanced by the constraint due to the additional load cell of Fig. 15. A schematic representation is illustrated in Fig. 16.

Fig. 16. Loads acting during the experimental testing.

In presence of a condition of horizontal chain, that can be realized employing no derailleur gear, and being the dimensions of the chain ring known, the real chain strength has been deduced and compared with the measurement of the proposed system.

The following table (Table II) contains the results of the experimental tests. In presence of an applied load on the pedals (first column), the real chain strength is derived by calculation (second column), the tyre- road interaction is measured by means of the auxiliary load cell (third column), and the measurement via the proposed system is obtained (last column).

TABLE II
EXPERIMENTAL RESULTS

Applied load (N)	Chain strength (N)	Tyre-road interaction (N)	Measurement (N)
21.6	43.2	5.9	34.3
31.4	62.8	7.8	48.1
41.2	82.4	9.81	63.8
60.8	121.6	13.7	94.2
80.4	160.9	17.6	125.6
109.9	219.7	23.5	173.6
129.5	259.0	27.5	206.0
158.9	317.8	34.3	257.0

In Fig. 17, the comparison between the sum T+Fx and the load cell measurement is reported.

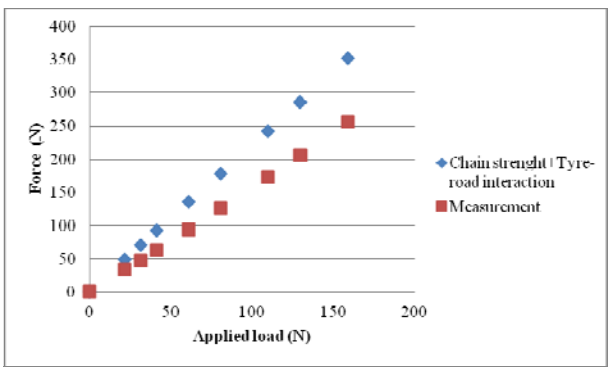

Fig. 17. Comparison between the load cell force and the force V.

Fig. 18 illustrates the measurement by means of the proposed system respect to the real chain strength for the several applied loads.

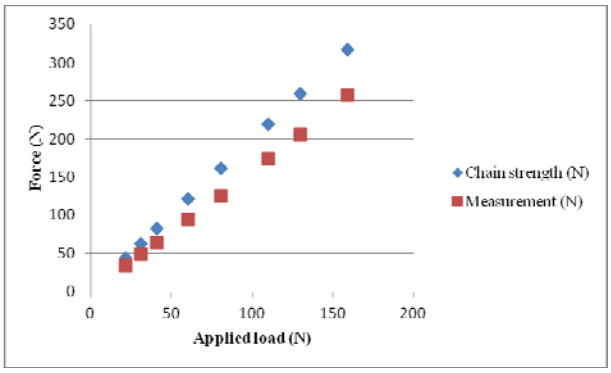

Fig. 18. Comparison between the chain strength and the measurement.

Figs. 17 and 18 show that the measurement by means of the proposed system gives an underestimation of the chain strength, differently from the theoretical results (Fig. 12). This difference can be determined by several causes, such as the presence of friction in the hinges and the presence of components of the chain strength that are balanced by the frame.

Fig. 19 confirms the linear behaviour concerning the input-output relationship of the measurement respect to the chain strength, as observed in the theoretical result (Fig. 13).

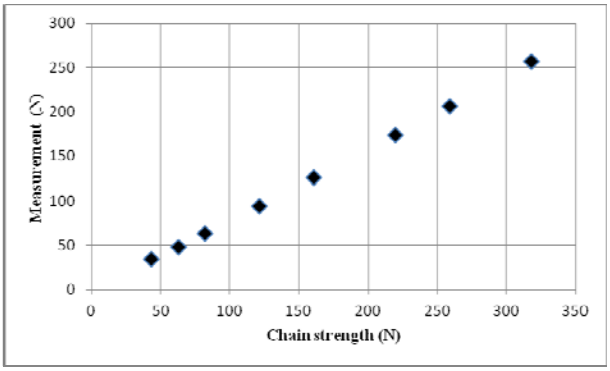

Fig. 19. Measurement vs real chain strength.

Fig. 20 shows the measurement error for the several values of the real chain strength.

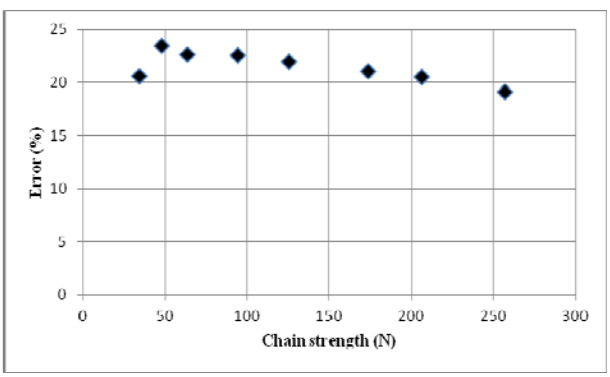

Fig. 20. Error vs real chain strength.

The obtained results highlight that the proposed measurement system gives as output a chain strength characterized by a value of about 20% lower than the real value. The repeatability of the measurement confirms the goodness of the proposed method, allowing an easy compensation of the measurement error. So, the results fully validate the proposed low cost method for the measurement of the chain strength in the electrically assisted bicycles.

VI. Conclusion

A low cost measurement system of the chain strength for electrically assisted bicycles has been proposed. It is functional for the feedback controlled bicycles whose assistance is proportional to the rider effort.

The system is based on the employment of a strain gauge load cell located between the rear wheel hub and the frame by means of suitable links. A theoretical and a numerical analysis have been presented in order to evaluate the forces acting on the proposed device and an experimental testing has been showed in order to validate it.

References

[1] T. Onoda and T. Gueret, "Fuel efficient road vehicle non-engine components: Potential saving and policy recommendations," *Int. Energy Agency Inf. Paper*, pp. 1–24, Oct. 2007

[2] P. Iodice, A. Senatore, "Experimental-analytical investigation to estimate an emission inventory from road transport sector,". *IAENG Transactions on Engineering Sciences - Special Issue of the International MultiConference of Engineers and Computer Scientists, IMECS 2013 and World Congress on Engineering*, WCE 2013, 2014, pp. 141-149.

[3] P. Iodice, A. Senatore, "Evaluation of Dispersion Models for Predicting Carbon Monoxide Concentrations from Motor Vehicles in a Metropolitan Area," *International Review on Modelling and Simulations*, vol. 6, no. 6, pp.1928 - 1932, 2013.

[4] H. Seki, K. Ishihara, and S. Tadakuma, "Novel regenerative braking control of electric power-assisted wheelchair for safety downhill road driving," *IEEE Trans. Ind. Electron.*, vol. 56, no. 5, pp. 1393–1400, May 2009.

[5] C. C. Tsai, H. C. Huang, and S. C. Lin, "Adaptive neural network control of a self-balancing two-wheeled scooter," *IEEE Trans. Ind. Electron.*, vol. 57, no. 4, pp. 1420–1428, Apr. 2010.

[6] A. Emadi, Y. J. Lee, and K. Rajashekara, "Power electronics and motor drives in electric, hybrid electric, and plug-in hybrid electric vehicles," *IEEE Trans. Ind. Electron.*, vol. 55, no. 6, pp. 2237–2245, Jun. 2008.

[7] A. Muetze and Y. C. Tan, "Electric bicycles: A performance evaluation," *IEEE Ind. Appl. Mag.*, vol. 13, no. 4, pp. 12–21, Jul./Aug. 2007.

[8] Y. Tanaka and T. Murakami, "A study on straight-line tracking and posture control in electric bicycle," *IEEE Trans. Ind. Electron.*, vol. 56, no. 1, pp. 159–168, Jan. 2009.

[9] M. Defoort and T. Murakami, "Sliding-mode control scheme for an intelligent bicycle," *IEEE Trans. Ind. Electron.*, vol. 56, no. 9, pp. 3357–3368, Sep. 2009.

[10] E. A. Lomonova, A. J. A. Vandenput, J. Rubacek, B. d'Herripon, and G. Roovers, "Development of an improved electrically assisted bicycle," in Conf. *Rec. IEEE IAS Annu. Meeting*, 2002, vol. 1, pp. 384–389.

[11] P. Fairley, "China's cyclists take charge: Electric bicycles are selling by the millions despite efforts to ban them," *IEEE Spectr.*, vol. 42, no. 6, pp. 54–59, Jun. 2005.

[12] N. Somchaiwong and W. Ponglangka, "Regenerative power control for electric bicycle," in Proc. *IEEE Int. Joint Conf. SICE-ICASE*, 2006, pp. 4362–4365.

[13] M. J. Yang, H. L. Jhou, B. Y. Ma, and K. K. Shyu, "A cost-effective method of electric brake with energy regeneration for electric vehicles," *IEEE Trans. Ind. Electron.*, vol. 56, no. 6, pp. 2203–2212, Jun. 2009.

[14] D. Schneider, "Easy rider: Convert your bicycle to a human–electric hybrid," *IEEE Spectr.*, vol. 46, no. 9, pp. 26–27, Sep. 2009.

[15] W. Du, D. Zhang, and X. Zhao, "Research on battery to ride comfort of electric bicycle based on multi-body dynamics theory," in Proc. *IEEE Int. Conf. Autom. Logistics*, Aug. 2009, pp. 1722–1726.

[16] S. Strano, M. Terzo, "A first order model based control of a hydraulic seismic isolator test rig," *Engineering Letters*, vol. 21, no. 2, pp. 52 – 60, 2013.

[17] F. Liccardo, S. Strano, M. Terzo, "Real-time nonlinear optimal control of a hydraulic actuator," *Engineering Letters*, vol. 21, no. 4, pp. 241 – 246, 2013.

[18] X-CELL RT, http://www.thun.de/en/products/sensor-technology/.

[19] TMM sensor, http://www.idbike.com/tmm-powermanagement.htm.